Application of a grid-scale lateral discharge model in the BALTEX region

STEFAN HAGEMANN* AND LYDIA DÜMENIL

Max Planck Institute for Meteorology
Bundesstraße 55
D-20146 Hamburg, Germany

*e-mail: Hagemann@dkrz.de
Tel.: +49 40 41173-101
Fax: +49 40 41173-366

WWW: http://www.mpimet.mpg.de/Depts/Modell/LSP

MPI-Report No. 278

October 1998

ISSN 0937-1060

Abstract

In this study, a hydrological discharge model is presented which may be applied as a tool to validate the simulation of the hydrologic cycle of atmospheric models that are used in climate change studies. It can also be applied in studies of global climate change to investigate how changes in climate may affect the discharge of large rivers.

The model was developed for the application with the climate models used at the Max-Planck-Institute for Meteorology. It describes the translation and retention of the lateral waterflows on the global scale as a function of the spatially distributed land surface characteristics which are globally available. Here, global scale refers to the resolution of 0.5˚ and lower, corresponding to a typical average gridbox area of about 2500 km^2. The hydrological discharge model separates between the flow processes of overland flow, baseflow and riverflow. The model parameters are mainly functions of the gridbox characteristics of topography and gridbox length.

The hydrological discharge model is applied to the BALTEX (Baltic Sea Experiment) region using input from an atmospheric general circulation model (ECHAM4) as well as from a regional climate model (REMO). The simulated inflows into the Baltic Sea and its sub-catchments are compared to observed and naturalized discharges. The results of this comparison are discussed and the simulated values of precipitation, surface air temperature and accumulated snowpack are compared to both observed data and surrogate data.

1. Introduction

A discharge model provides a useful tool for the validation of atmospheric models. For the application with the climate models used at the Max-Planck-Institute for Meteorology, a model was developed (*Hagemann and Dümenil*, 1998) which describes the translation and retention of the lateral waterflows on the global scale as a function of spatially distributed land surface characteristics which are globally available. Here, global scale refers to the resolution of 0.5˚ and lower, corresponding to a typical average gridbox area of about 2500 km^2. At this scale some aspects of land surface characteristics are available as datasets of global coverage. The scale of 0.5˚ is also a good compromise between the macroscale of the atmospheric general circulation models (GCMs) and the comparatively small scale hydrological processes.

A global discharge model is sufficient for applications using input from climate models the resolution of which is often coarser than 0.5˚. For the more detailed simulation of discharge of a specific river in conjunction with input from high-resolution hydrological models, catchment related discharge models may be applied but these have to be gauged with measured data.

Some basic information about lateral discharge and its flow processes as well as a description of the global discharge model are presented in Sect. 2.

This study focuses on the BALTEX (Baltic Sea Experiment) region. BALTEX is a European sub-program of the 'Global Energy and Water Cycle Experiment' (*WMO*, 1988) covering the Baltic Sea catchment (cf. *BALTEX*, 1995). In this region hydrological data are available at high spatial and time resolution.

In the BALTEX region, the discharge model was used as a tool to investigate the performance of two different atmospheric circulation models with different model resolutions. With respect to this purpose, we consider the atmospheric GCM ECHAM4 (*Roeckner et al.*, 1996) at T42 resolution (corresponds to a spatial resolution of about 2.8˚) and the regional climate model REMO (*Jacob and Podzun*, 1997) using the physical parameterization package of the German Weather Service (DWD, see also Sect. 3.2) and a rotated 0.5˚ grid for spatial resolution. Sect. 3 gives a short overview about the hydrological representation of the soil in the two models.

The simulated inflows into the Baltic Sea and its sub-catchments are then compared to observed discharges (*Bergström and Carlsson*, 1993). These comparisons are presented in Sect. 4.

The results from these comparisons are discussed in Sect. 5. Here, the simulated values of precipitation, surface air temperature and accumulated snowpack are compared with both observed data and surrogate data generated by the HBV model (Bergström *et al.*, 1996).

2. The discharge model

Sect. 2.1 provides some basic information about lateral flow processes. In Sect. 2.2, the technical details and the structure of the HD model are presented.

2.1. Lateral waterflow

The lateral waterflow on the global scale is composed of several flow processes. We distinguish between water produced within a catchment or gridbox, and water entering the catchment from other catchments through the boundaries.

Water which originates within the catchment may contribute to the flow processes in different ways. If water reaches the land surface by throughfall (the amount of rain which reaches the soil) or snowmelt, it may infiltrate into the soil or may flow laterally as surface flow. Water in the upper soil layers may evaporate, percolate downwards or may flow laterally as interflow. Water in the deep soil layers may rise again by capillary forces or may flow laterally as baseflow. The influence of the first process is negligible on the global scale. In hydrology surface flow and interflow are usually merged into overland flow (*Miller et al.*, 1994). Occasionally, hydrologists use the terms fast and slow flow which are nearly the same as overland flow and baseflow.

The lateral waterflow between different catchments is transferred by the river network and is referred to as riverflow. For catchments having inflow from other catchments, the riverflow is often the main flow process provided that the amount of water from the inflow is large compared to the amount of the lateral waterflow which originates from inside the catchment. For many other catchments overland flow is the dominant flow process, especially if snowmelt plays an important role in the hydrological cycle. Baseflow often is responsible only for a slowly changing part of the discharge, which is distinguishable only in a discharge curve either during the winter in catchments where the soil is frozen, or in dry regions where precipitation events occur rarely.

At the spatial resolution of 0.5˚, which corresponds to an average distance of about 55 km, the riverflow has typical lag times of a few days, the overland flow has lag times ranging from several days to a few weeks, and the baseflow lag times range between a few months and several years.

2.2. The HD model

Fig. 1 shows the model structure of the Hydrological Discharge model (*Hagemann and Dümenil*, 1998) that will be referred to as HD model in the following. It separates the lateral waterflow into the three flow processes of overland flow, baseflow and riverflow. Overland flow and baseflow are both represented by a single linear reservoir, and riverflow is represented by a cascade of *n* equal linear reservoirs (In *Hagemann and Dümenil* (1998) overland flow was also represented by a reservoir cascade but more recent results (*Hagemann*, 1998) have shown that the representation of a single linear reservoir is sufficient for a global discharge model.). Overland flow uses runoff as input, baseflow is fed by drainage and the inflow from other gridboxes contributes to riverflow. The sum of the three flow processes equals the outflow from a gridbox.

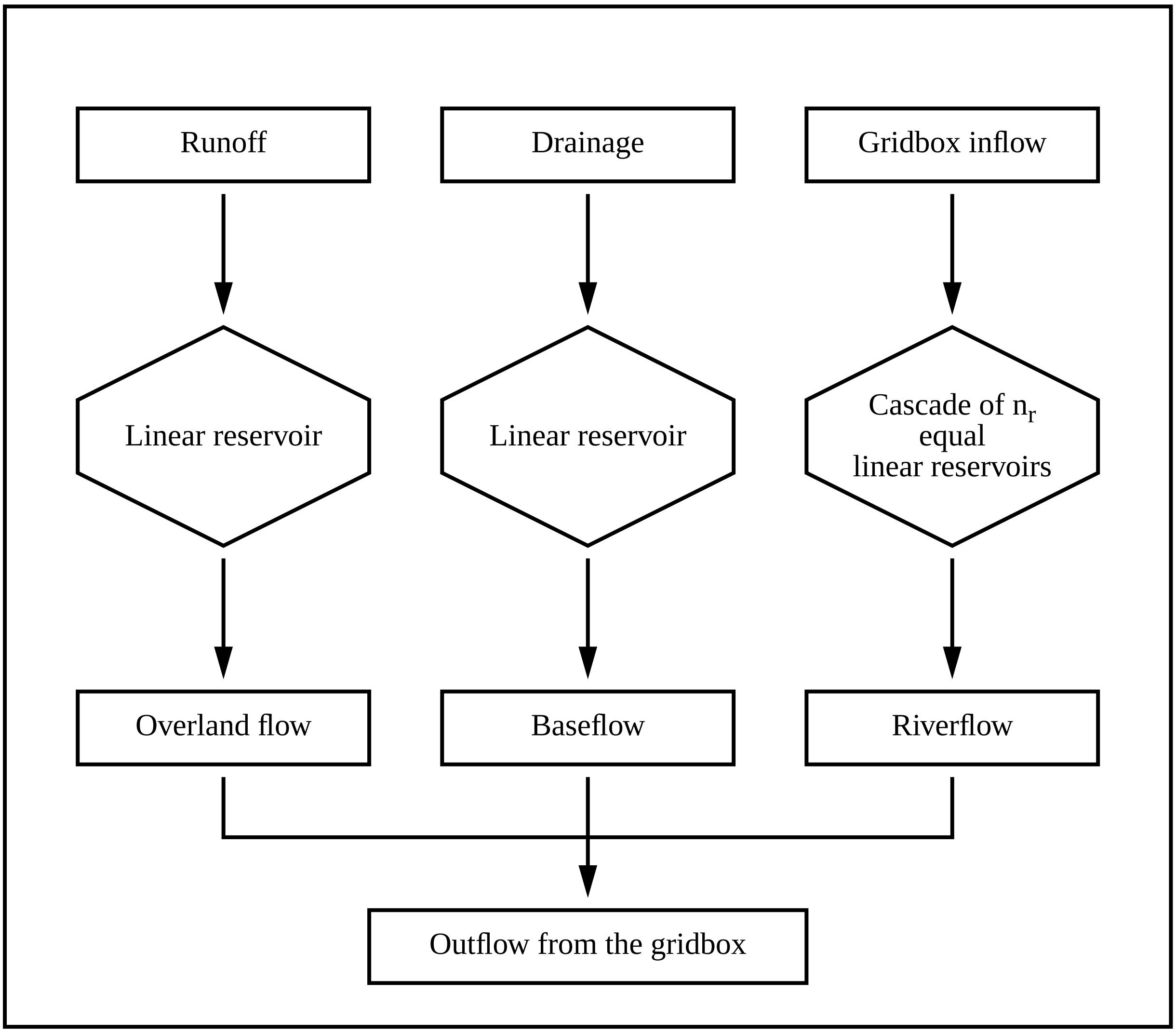

Fig. 1: Structure of the HD model

For overland flow, the retention coefficient k_o of the linear reservoir is a function of the average slope within a gridbox and the gridbox length Δx. The gridbox length is defined as the distance between the centres of two adjacent gridboxes in the direction of the flow. For riverflow, the retention coefficient k_r of the linear reservoirs is a function of the topography gradient Δh between two adjacent gridboxes in the direction of the flow and the gridbox length Δx. The parameters of overland flow and riverflow are influenced by the wetland fraction and the lake area within a particular gridbox (see *Hagemann and Dümenil*, 1998b). The retention time k_g of the baseflow reservoir is a function of the gridbox length. Its value for a typical 0.5˚ gridbox (Δx = 55 km) was set to 300 days. Here, the exact typical value of k_g is not very important because the HD model is not very sensitive to small changes in k_g.

As a general strategy the HD model computes the discharge only at 0.5˚ resolution. All model input fields (such as runoff and drainage) from the various GCM resolutions are therefore interpolated to the same 0.5˚ grid. The HD model uses a daily time step. Only for riverflow the time step is six hours to pay regard to the minimum travel time through a 0.5˚ gridbox which is limited by the time step chosen.

For each gridbox of the HD model eight possible outflow directions (the four main directions North (N), East (E), South (S) and West (W) and the four diagonal directions NE, SE, SW and NW) are defined, but for a specific gridbox only one outflow direction is permitted. The outflow from this gridbox enters the neighbouring gridbox which has the lowest topography value of the surrounding gridboxes.

The skill of the discharge simulation depends not only on the formulation of the model equations, but also on the precise definition of the boundaries of the model catchments. The sizes and the positioning of the model catchments on the globe were defined by using a modified topography dataset. Since the definition of flow directions derived from the available 0.5˚ topography dataset[1] is not detailed enough for an accurate global discharge simulation, a model topography had to be created. Several mathematical methods (cf. *Hagemann and Dümenil*, 1998) were developed to include important aspects of the real topography such as river flow paths and catchment borders which cause a good agreement between the model catchments and the real catchments. This agreement is generally not perfect because the methods used are automated to a certain degree. Pure manual methods would give a perfect agreement globally but they are too expensive and will not considerably improve the simulation of discharge.

1. The available global 0.5˚ topography dataset was derived from the global five minute topography data-set of the National Geographic Data Centre (*Edwards*, 1989) by area weighted averaging.

3. Atmospheric model simulations

The HD model represents the water fluxes between the land surface and the ocean. It is designed for the use in a coupled GCM. But in the off-line mode it can be applied to the output of every climate model desired as it is done in this study to ECHAM4 (*Roeckner et al.,* 1996) and REMO (*Jacob and Podzun*, 1997) model simulations.

The land surface parameterizations of the ECHAM4 and REMO with DWD physics are quite different. Among others this is particularly true for the representation of the soil processes. In Sect. 3.1 some characteristics of the soil and the generation mechanisms of runoff and drainage of ECHAM4 are presented. In Sect. 3.2 this is repeated for REMO.

3.1. ECHAM4

In ECHAM4 the soil is represented by a single soil layer. Time series of runoff and drainage are calculated according to the scheme of *Dümenil and Todini* (1992). Here, runoff is computed as infiltration excess from a bucket which takes the subgrid variability of the soil saturation within a GCM gridbox area into account. This is done by defining a statistical distribution of soil water capacities in the gridbox (*Roeckner et al.*, 1992). This means that runoff may occur after a rainfall event even if the whole gridbox is not yet saturated. Drainage is the amount of water which is allowed to percolate downwards from the bucket.

In the global application of the HD model, the input fields of runoff and drainage are taken from an uncoupled atmospheric ECHAM4-T42[1] control simulation using climatological sea surface temperature (SST). For this control simulation daily values of runoff and drainage are available for five years. As mentioned above the input values were transformed from the T42 grid to a 0.5˚ grid.

3.2. REMO

In a comparison of a regional climate model to a GCM, it would be desirable (e. g. for the investigation of scaling effects) to use models which use the same parameterizations in the soil but unfortunately for the version of REMO with ECHAM4-physics only short time simulations exist at the time of the writing (*Jacob*, 1998, personal communication). The effects of initialization errors, interannual variability and storage differences in the atmospheric model as well as in the discharge model can be minimized by performing model simulations for several years. Therefore a model version of REMO is used which includes the physical parameterization package of the German Weather Service[2] which is almost identical to the Europamodell/Deutschlandmodell system (*Majewski and Schrodin*, 1994).

---

1. ECHAM4 is the currently operational version of the atmospheric GCM used at MPI. T42 describes the model resolution which equals a horizontal grid length of about 2.8˚.
2. This is the package version of May 1995. Since then only minor changes were made. (*Jacob and Podzun*, pers. comm., 1998). Also the handling of the spatial boundary forcing was changed which has effects in the boundary zone of the model region. (The Baltic Sea catchment is not located in this boundary zone.)

This REMO version contains a different hydrological representation than ECHAM4. Here, the soil is divided into three hydrological soil layers. Vertical moisture transport follows the Darcy equation for one-dimensional fluid flow (e. g. *Roesch et al.*, 1997) which includes the influence of gravity and capillary forces. If water reaches the soil surface, either as snowmelt or coming from an interception reservoir, it may infiltrate or flow off as surface runoff if the upper soil layer is saturated. Drainage from the soil may occur from each of the three soil layers if its water content is larger than its porosity.

For the application of the HD model, daily input values of runoff and drainage are taken from an available four years REMO simulation. With regard to the spatial resolution, REMO uses a rotated[1] 0.5˚ grid, so that the input values had to be transformed into the regular 0.5˚ grid, too. The REMO model region was nested into a T42 grid and the forcing through the boundaries of this region was generated by the atmospheric GCM ECHAM3-T42 (*Roeckner et al.*, 1992) using observed SST from the years 1979-1982. These spatial boundary conditions were updated every 6 hours and they were linearly interpolated in between the update times as REMO operates with a five minute time step.

1. The rotated 0.5˚ grid was created from a regular grid by shifting the equator into the centre of the considered model region to accomplish that the gridboxes of the whole region have similar area sizes.

4. Application to the BALTEX region

At a first glance the observational river gauge data seem to be a useful tool for the validation of simulated discharges. Unfortunately many rivers are anthropogenically influenced so that the measured discharge is not in agreement with the natural flow characteristics of the river. As an alternative, naturalized flows may be used, but these are only available for a few catchments, e.g. in Sweden (*Bergström et al.*, 1993) and other parts of Scandinavia (*Bergström*, 1995, personal communication). In order to compute the naturalized flows, detailed information about the anthropogenic influences is needed, such as the regulation characteristics of storage reservoirs and large dams, the influences of power plants or the regulation mechanisms of irrigation systems. This information is required for meaningful studies of global change, but at present it is not available for the whole globe.

Thus the validation of a global discharge model is in principle restricted to catchments where the rivers are unregulated or the naturalized flow can be estimated. But at the current state of development the difference between simulated and observed discharges is often larger than the deviation between measured and naturalized flows since in the simulated discharge the sum of errors of both the atmospheric and the discharge model may become visible. For some heavily regulated rivers the deviations between observed and naturalized flows may be very large, so that for those rivers a global discharge simulation will not totally agree with the present day discharge data. The differences between naturalized and observed discharges occur mainly in the annual cycle, while the differences in the year-to-year management of total volumes of discharge are comparatively small.

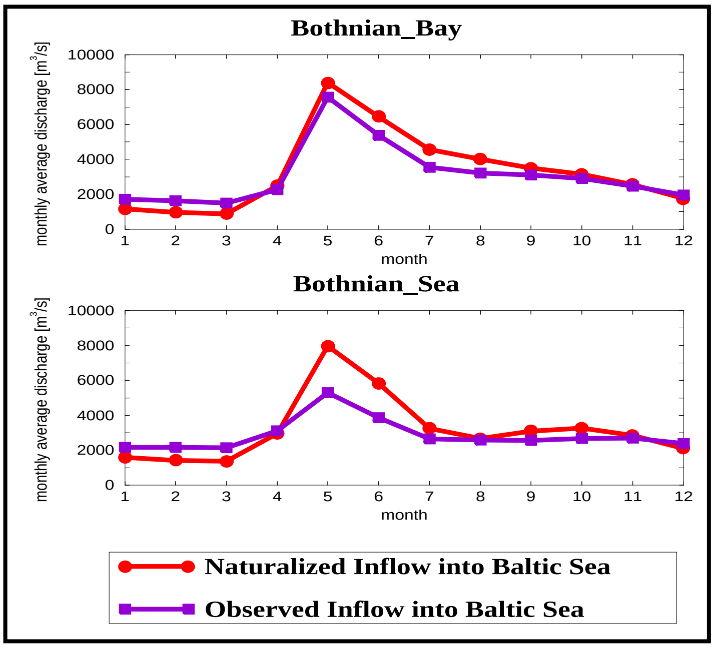

Fig. 2: Comparison of naturalized and observed inflow into the Bothnian Bay and Bothnian Sea.

For our comparisons in the Baltic Sea catchment we focus on the sub-catchments of Bothnian Bay and Bothnian Sea which are located in the northern part of the Baltic Sea catchment. For these two catchments, naturalized inflow data exist, and they are compared with observed inflow data in Fig. 2. The difference between the naturalized and the observed inflow is almost negligible for the Bothnian Bay, while there is a significant discrepancy between the annual cycles of monthly mean inflow for the Bothnian Sea catchment.

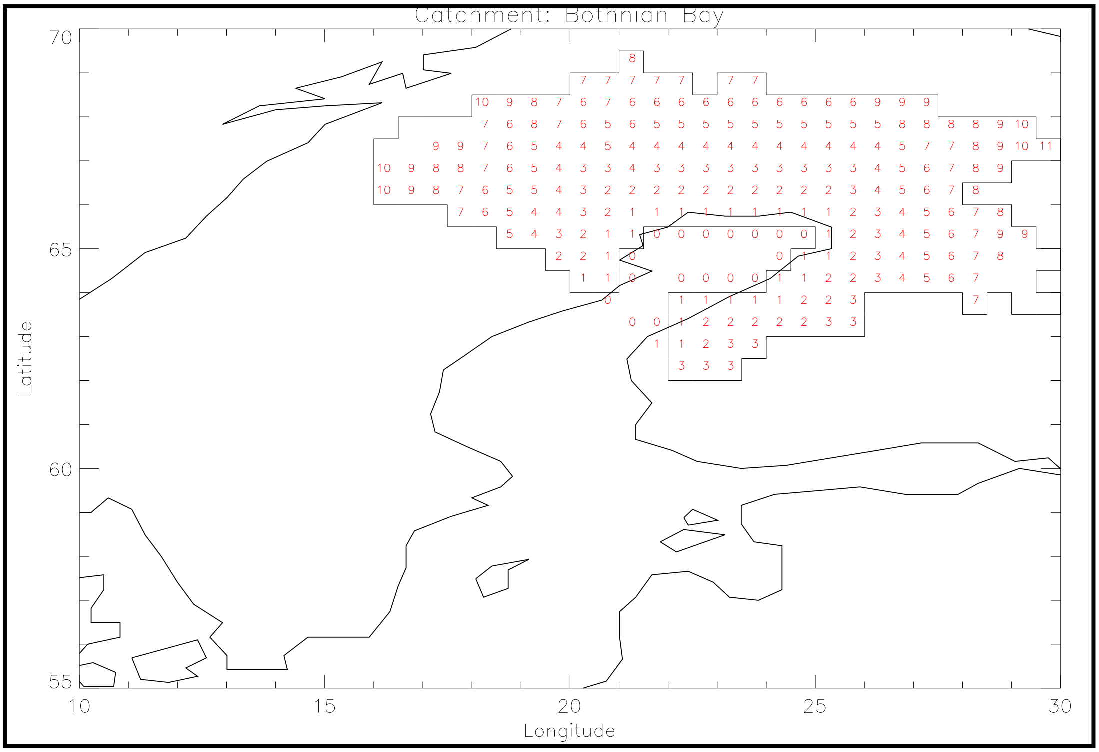

Fig. 3: Bothnian Bay. The numbers correspond to the gridboxes of the model catchment and express the flow distance in gridboxes from the inflow box (= 0) into the Baltic Sea. The thick line represents the border of the real catchment derived from a dataset (*Hagemann and Dümenil*, 1998).

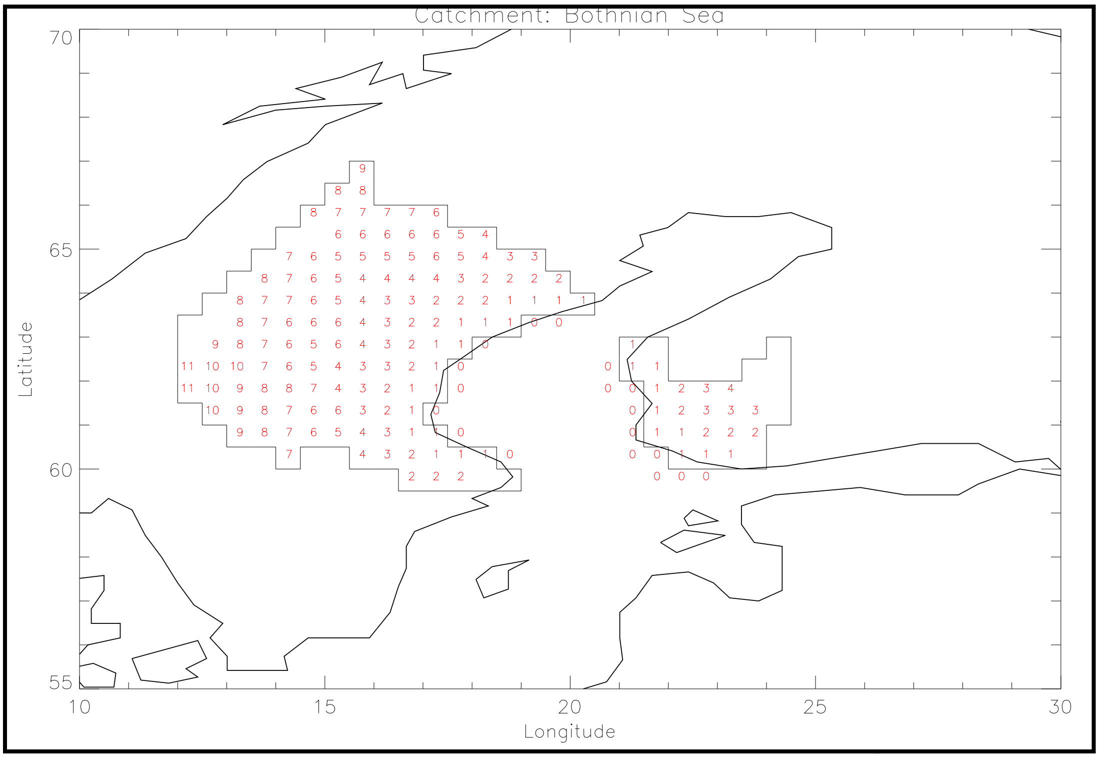

Fig. 4: Bothnian Sea. The numbers correspond to the gridboxes of the model catchment and express the flow distance in gridboxes from the inflow box (= 0) into the Baltic Sea. The thick line represents the border of the real catchment derived from a dataset (*Hagemann and Dümenil*, 1998).

Fig. 3 and Fig. 4 show the model catchments and the real catchments of these two regions. Although both model catchments agree well with their corresponding real catchments, there are still some small differences (cf. Sect. 2.2) which have to be considered when discharge volumes are investigated.

4.1. Observed data

We compared the simulated discharge from both atmospheric models with the observed discharge. Unfortunately the output of these models belongs to different time periods. The ECHAM4 run was forced by climatological SSTs so that the simulated atmospheric values should be representative for climatological conditions. Therefore we should compare its output to averaged values derived from long time series of measured discharge. The four years of REMO output should correspond directly to the years 1979-1982 since the GCM that forces REMO through the spatial boundaries uses the SST of this period (cf. Sect. 3.2). Here, one has to bear in mind that the inter-annual variability at middle- and high-latitudes is strongly dominated by chaotic dynamics, so that the tropical SST forcing only modulates the atmospheric circulation (*Bengtsson et al.*, 1996). Due to the natural annual variability the REMO four year mean values as well as the ECHAM4 five year mean values may differ from the long term averages.

Table 1 presents catchment areas and discharges of the Baltic Sea and the two Bothnian sub-catchments. The observed volumes of discharge are shown separately for the long time period of 40 years and for the four years 1979-1982. In the two Bothnian sub-catchments the discharge amounts are the same for both periods, but the inflow into the total Baltic Sea in the four year period is about eight percent higher than that of the whole 40 year period.

Table 1: A selection of observed characteristics of the considered Baltic catchments. The discharge amounts in mm/year are averaged over the corresponding catchment area. The naturalized flows are recalculated from the observed discharges by *Bergström et al.* (1993).

	Bothnian Bay	Bothnian Sea	Baltic Total
Catchment area (real)	261 000 km^2	230 000 km^2	1729 000 km^2
Discharge: 1950 - 1990	98 km^3/year 375 mm/year	90 km^3/year 391 mm/year	483 km^3/year 279 mm/year
Discharge: 1979 - 1982	99 km^3/year 379 mm/year	91 km^3/year 396 mm/year	523 km^3/year 302 mm/year
Naturalized flow: 1981 - 1991	105 km^3/year 402 mm/year	84 km^3/year 365 mm/year	--

In order to compare the annual cycles of simulated and measured inflow into the Baltic Sea we use the naturalized inflow instead of the observed one, as mentioned before (Sect. 4). Note that data of naturalized inflow are available only for the years 1981-1991 yielding a somewhat different amount of discharge compared to the discharge of the other time periods.

4.2. Atmospheric model output

In this section we consider the amount of water which is produced by the atmospheric models as the sum of runoff and drainage which we denote as W_{RD} in the following.

The HD model uses a regular grid with a resolution of 0.5˚. Therefore the atmospheric model output W_{RD} is transformed from its original resolution to this resolution. At the 0.5˚ resolution we use a distribution of catchments over land which is taken from a modified version (*Hagemann and Dümenil*, 1998) of a dataset of the *US Army Corps of Engineers* (1994). In this dataset the real catchments are digitized so that the catchment areas do not exactly agree with the real areas although the differences are very small. The gridded areas are shown in Table 2. Area coverage indicates the fraction of gridded area divided by the real area taken from *Bergström and Carlsson* (1993).

Now we can compute W_{RD} inside the gridded catchments and compare it to the observed discharge. If not stated otherwise the comparisons for ECHAM4 and REMO are done for their corresponding time periods (see Sect. 4.1). Table 2 shows that for ECHAM4 the amount of W_{RD} agrees quite well with the observed discharge volumes in the Bothnian sub-catchments whereas in the total Baltic Sea catchment this amount is somewhat larger than the observed discharge.

Table 2: Atmospheric model simulated discharge (= W_{RD}) on the 0.5˚ grid. The discharge amounts in mm/year are averaged over the corresponding catchment area. Area fraction designates the ratio of the 0.5 degree catchment area and the real observed area shown in Table 1.

	Bothnian Bay	Bothnian Sea	Baltic Total
Area (0.5˚ dataset)	276 884 km^2	234 748 km^2	1777 757 km^2
ECHAM4: Runoff + Drainage (W_{RD})	97 km^3/year 350 mm/year	92 km^3/year 392 mm/year	524 km^3/year 295 mm/year
REMO: Runoff + Drainage (W_{RD})	134 km^3/year 484 mm/year	105 km^3/year 447 mm/year	546 km^3/year 307 mm/year
Area fraction	106%	102%	103%
ECHAM4 / (1950-90 discharge)	93%	100%	106%
REMO / (1979-82 discharge)	128%	113%	102%

Contrary to this, REMO produces too much W_{RD} in all catchments, especially in the Bothnian Bay the amount of W_{RD} is particularly high with an overestimation of 35% compared to the observed discharge.

4.3. Simulated discharge

As mentioned before in Sect. 4 the model catchments differ from the real catchments. This difference is small for the Bothnian Bay, but the model catchment of the Bothnian Sea is comparatively smaller than the real one, while the model catchment of the total Baltic Sea is a little larger than in reality. Therefore differences between the volumes of simulated discharge and observed discharge occur which we must take into account when we consider the annual cycles in Sect. 4.4, especially for the Bothnian Sea. Table 3 shows statistics of the simulated discharge for the model catchments. Area fraction indicates the fraction of model catchment area divided by the real area.

Table 3: Simulated discharge using the HD Model. The discharge amounts in mm/year are averaged over the corresponding catchment area. Area fraction designates the ratio of the model catchment area and the real observed area shown in Table 1.

	Bothnian Bay	Bothnian Sea	Baltic Total
Area (HD model catchment)	265 585 km^2	209 163 km^2	1790 808 km^2
ECHAM4 --> Simulated discharge	94 km^3/year 354 mm/year	84 km^3/year 402 mm/year	525 km^3/year 293 mm/year
REMO --> Simulated discharge	126 km^3/year 474 mm/year	93 km^3/year 445 mm/year	540 km^3/year 302 mm/year
Area fraction	102%	91%	104%
ECHAM4_HD / (1950-90 discharge)	94%	103%	105%
REMO_HD / (1979-82 discharge)	125%	112%	100%

4.4. Annual cycles

In this section the annual cycles of W_{RD} and the corresponding simulated discharge Q_{sim} are compared to the naturalized inflow into the Bothnian Bay and Bothnian Sea.

Fig. 5 shows results for ECHAM4. The inflow into the Bothnian Bay is simulated well, but there is too little discharge during the summer. For Bothnian Sea the snowmelt induced discharge peak in spring is simulated too early. This may be based on a erroneous handling of the snowmelt parameterization in ECHAM4 or on a wrong retention of the water by the HD model in this region. Generally too little volume of the flow is generated which may be mainly based on the smaller area of the model catchment of the Bothnian Sea.

Fig. 6 shows W_{RD} and Q_{sim} for REMO. For both catchments, the discharge peak in spring is simulated too late, although the delay for Bothnian Sea is not very large. Again the late discharge peak may be based on errors of REMO or of the HD model. For Bothnian Sea, there is also too less flow during summer.

Fig. 7 compares the atmospheric model output W_{RD} from both models which is the input for the HD Model. For Bothnian Bay both models show different behaviour in June/July, for Bothnian Sea there are differences in March as well as in June/July. These curves reveal that in ECHAM4 the snowmelt is simulated almost one month earlier for both catchments.

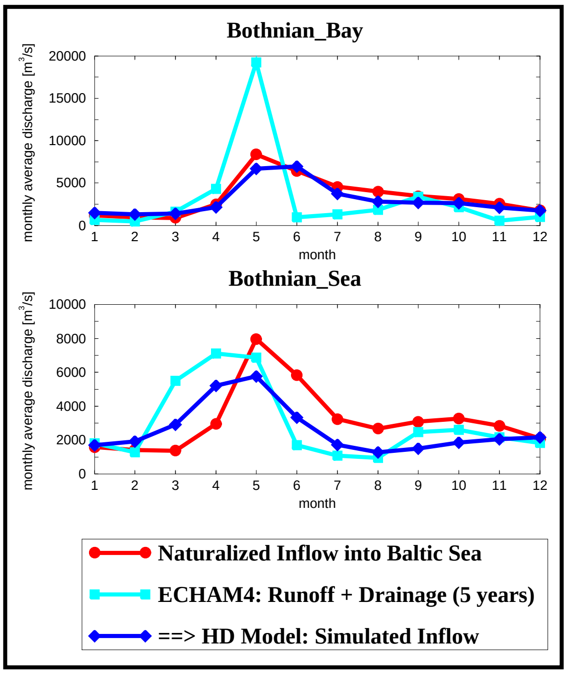

Fig. 5: ECHAM4: W_{RD} and simulated inflow compared to the naturalized inflow

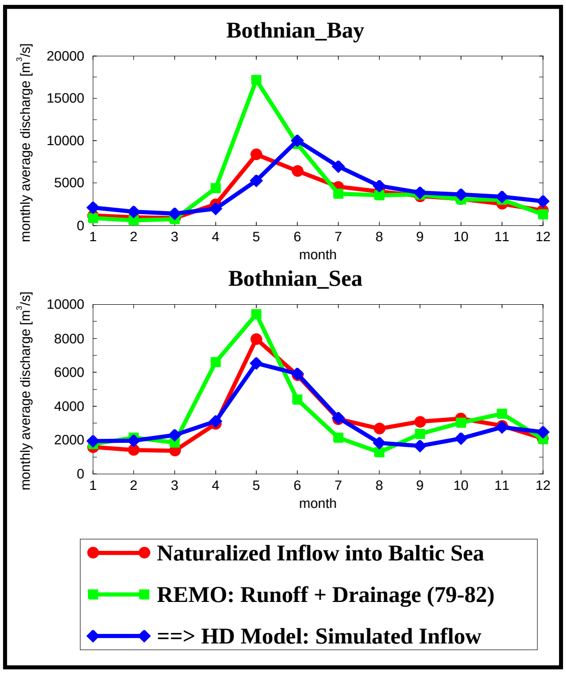

Fig. 6: REMO: W_{RD} and simulated inflow compared to the naturalized inflow

These differences in the input of the discharge simulation yield the curves shown in Fig. 8. Their differences may be due to the varied qualitative behaviour of the atmospheric models in both catchments or may be also based on different flow characteristics in these two regions which can not be simulated properly by the HD model.

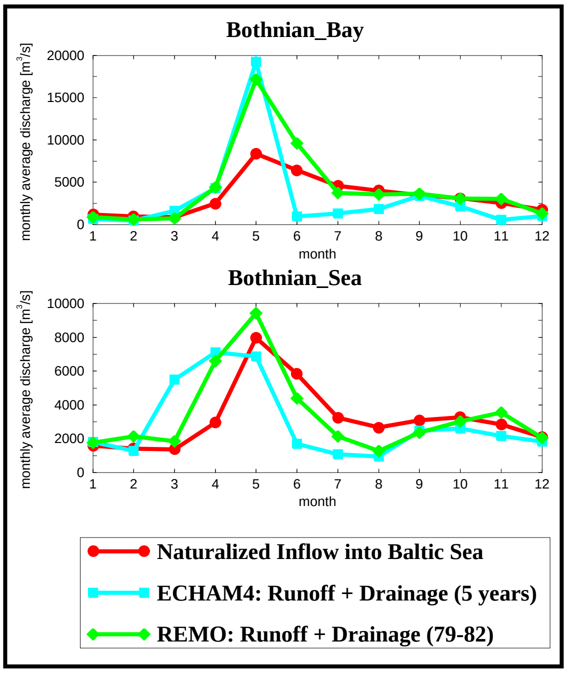

Fig. 7: Comparison of W_{RD} and naturalized inflow

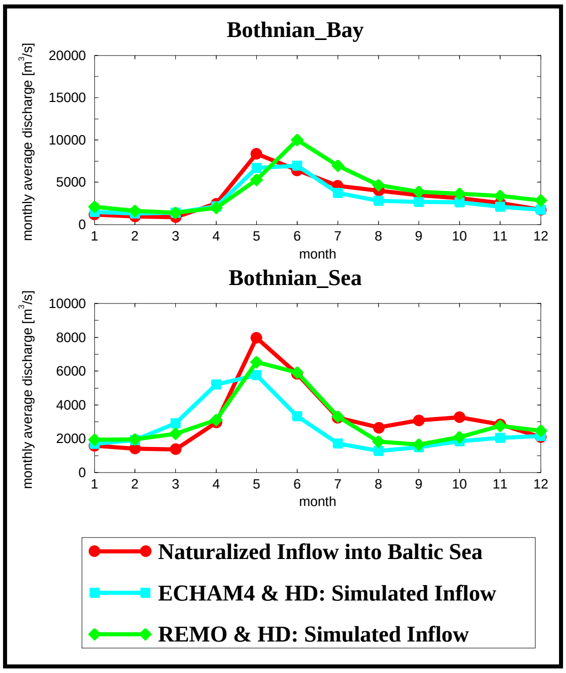

Fig. 8: Comparison of simulated and naturalized inflow

5. Discussion

The discharge curves presented in Sect. 4.4 show a different behaviour. Possible deficiencies of the atmospheric models are added to possible weaknesses of the HD model so that the sum of all possible errors may become visible in the simulated discharge. From the discharge curves alone we cannot decide whether the time delay of the snowmelt in spring is caused by REMO or by the HD model. It should be expected that REMO can simulate the regional climate better than ECHAM4 due to its much finer spatial resolution. But we must bear in mind that its spatial boundary conditions are defined by ECHAM3, so that errors in these boundary conditions may be transported into the climate patterns of the REMO region. In order to consider the causes of the different behaviour of the discharge curves we have compared several simulated hydrological values and 2m temperatures with observations.

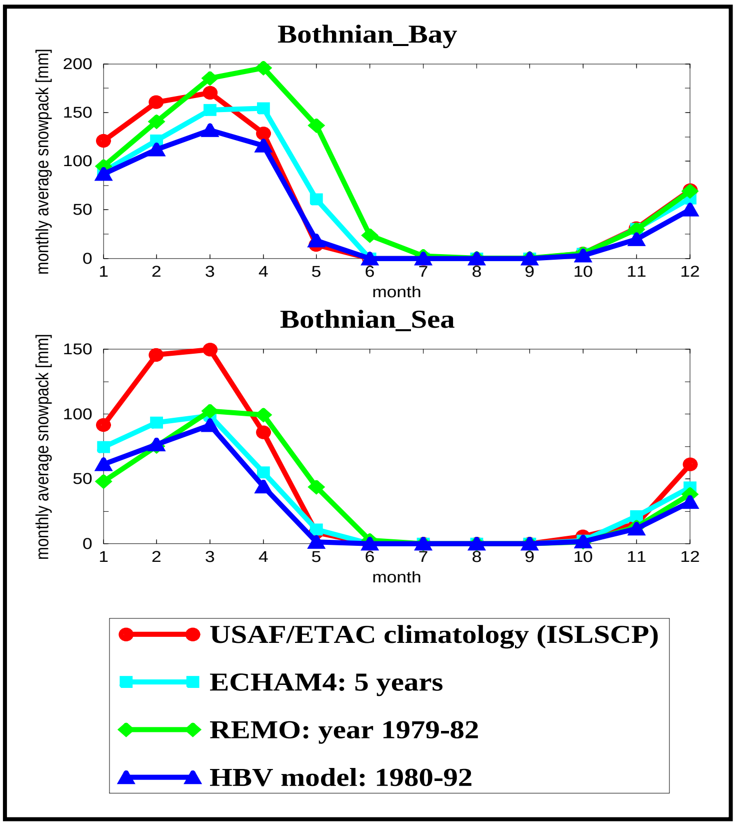

Fig. 9: Comparison of simulated and observed accumulated snowpack

Fig. 9 shows observed and simulated annual cycles of the accumulated snowpack. As observed snowpack we use the snow data climatology (*Foster and Davy*, 1988) and the snowpack simulated by the HBV model (*Bergström et al.*, 1996) for the years 1980-92 which can be viewed as surrogate data. For Bothnian Bay, both climate models compute the time of the snowmelt in spring too late compared to the two observed curves. For REMO there is a delay of about 1 month, while for ECHAM4 this delay is about 10 days and may be within the accuracy of the observed data. This agrees well with our investigations of the simulated discharge curves, and indicates that the late discharge peak in spring is based on deficiencies of the REMO simulation for this region.

For Bothnian Sea, REMO computes the time of the snowmelt one-third of a month later than the snow data climatology and one month later than the HBV model. ECHAM4 simulates the time of the snowmelt about a half month earlier than the snow data climatology and agrees with the HBV model. Again these results agree with our discharge investigations. For both regions, REMO is simulating the snowmelt too late as concluded from the discharge curves. ECHAM4 computes the time of the snowmelt quite well, although for Bothnian Sea this occurs a little too early. Since the time of the snowmelt of the HBV model agrees with ECHAM4, it seems that the HBV model has also small deficiencies for this region.

The underestimation of the 2m-temperature seems to be the main reason for the late snowmelt of REMO. This can be seen in Fig. 10, where the simulated 2m-temperatures are compared to synoptic temperature data (*Bergström et al.,* 1996) from 1980-92 and the climatology of *Legates and Wilmott* (1990). In spring for both catchments, the simulated temperature curve of REMO reaches temperatures above the freezing point about one month later than the observed ones. In addition to this, the temperature is mostly too cold during the whole year. ECHAM4 agrees quite well with both observations.

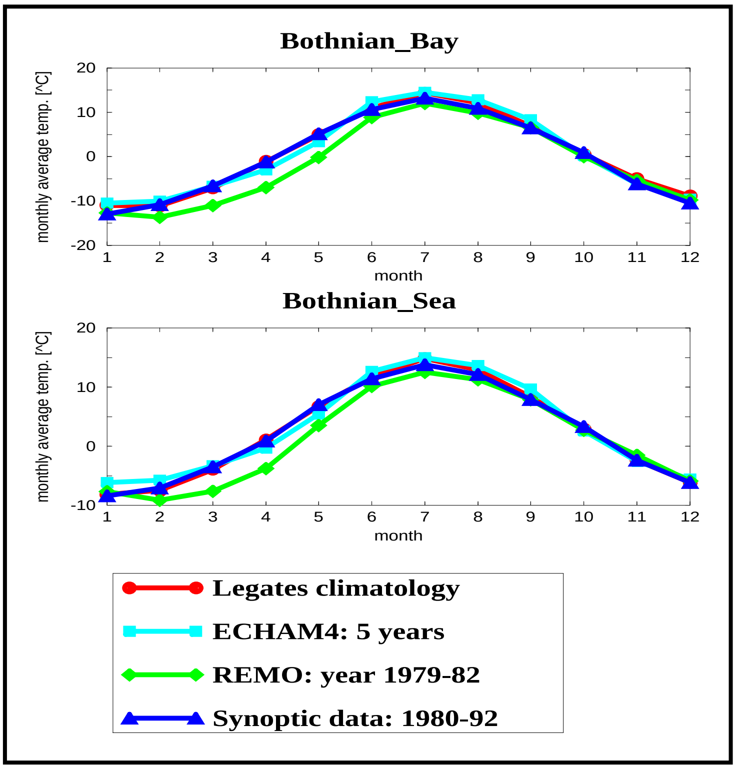

Fig. 10: Comparison of simulated and observed 2m-temperature

Christensen et al. (1998) found out that in their studies with a very high resolution (19 km) limited area model (HIRHAM4; *Christensen et al.* 1996) over Scandinavia, the surface air temperature was underestimated for all seasons resulting in a delayed snowmelt in spring. This was explained by problems in the general circulation in the winter season, but not in the other seasons. As an explanation it was suggested that especially efficient land sea-breeze systems developed in their very high resolution simulation in the warm part of the year which transported cold air from the surrounding sea to the land areas and, thus, cools down the land surface too strong.

Fig. 11 shows the simulated precipitation curves compared with synoptic precipitation data (*Bergström et al.*, 1996) from 1980-92 and the climatology of the GPCP[1] (*Rudolf et al.*, 1996). For both catchments, ECHAM4 simulates too much precipitation except during summer (July/ August) where too little precipitation is simulated. For the Bothnian Bay, REMO simulates also too much precipitation, especially during late spring (May/June), but the amount is not less than the observed values in any month. For Bothnian Sea, REMO behaves in a similar way, but in August there is much lesser precipitation than observed. Its amount is actually lesser than the value of ECHAM4. The underestimated summer precipitation of both atmospheric simulations in the Bothnian Sea has an obvious effect on the simulated discharge (see Fig. 8) which is also too low in the summer.

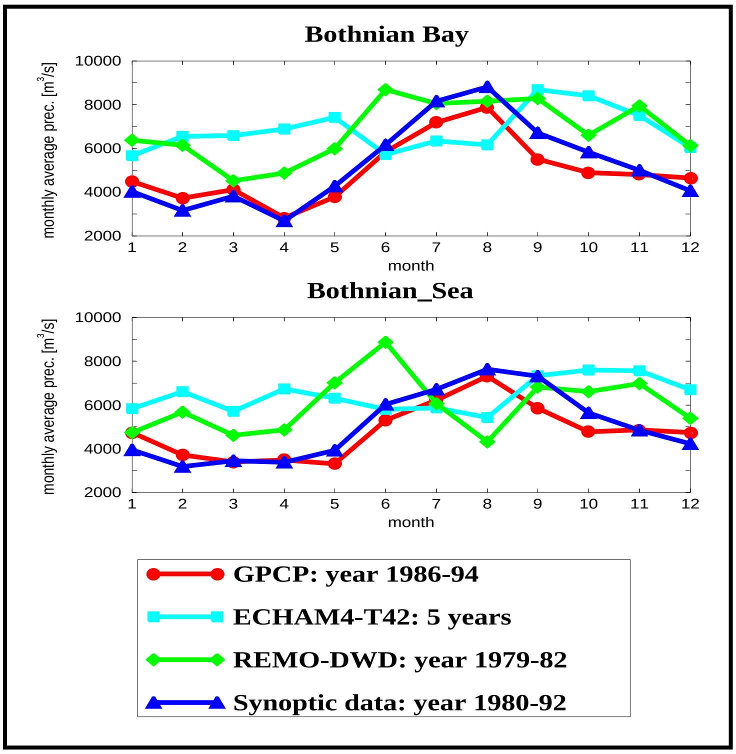

Fig. 11: Comparison of simulated and observed precipitation

Machenhauer et al. (1996, 1998) validated several global and regional climate models over Europe (among others ECHAM4 and HIRHAM4) and found that errors in the near surface general circulation, corresponding to systematic errors in the mean sea level pressure fields, seem to explain significant biases in the primary weather elements, especially in precipitation. For simulations with ECHAM4 and HIRHAM4 at high (50 km) and very high resolution, this was discussed in more detail for Scandinavia by *Christensen et al.*, (1998). Of course, systematic errors in the precipitation will lead to errors in the simulation of the hydrological cycle.

For a specific region, the continuity equation is valid at the land surface:

1. GPCP = Global Precipitation Climatology Project

$$\frac{dS}{dt} = P - E - W_{RD} \tag{1}$$

dS/dt is the change in time *t* of the total volume of water that may be stored at the land surface, *P* is the precipitation, and *E* is the evapotranspiration. For larger areas and longer time periods (such as a year) observations have shown that *dS/dt* is small compared to the other terms of Eq. (1) (*Peixoto*, 1993). Thus, Eq. (2) is valid for the long term annual means in a large catchment with the discharge *Q*:

$$P - E = W_{RD} = Q \tag{2}$$

From the annual means of precipitation, which are larger than observed for both climate models, it is expected that the simulated discharges (cf. sum of runoff and drainage in Table 2) should also be larger than observed. This is the case for REMO, but not for ECHAM4, where the amounts of runoff + drainage agree well with the observed discharges. Since Eq. (2) should be valid for the five years of the ECHAM4 simulation, this leads to the conclusion that ECHAM4 computes too much evapotranspiration for both catchments. *Wild et al.* (1996) stated that ECHAM4 would compute realistic surface fluxes if the land surface gets the correct atmospheric forcing. Thus, the overestimation of evapotranspiration seems to be caused by deficiencies in the atmospheric part of ECHAM4.

Slighter differences between observed and simulated hydrological values may occur, because of the different time periods used for the simulations and some observations.

6. Conclusions

The HD model performs well for the two Baltic sub-catchments of Bothnian Bay and Bothnian Sea. From the atmospheric REMO simulation, too much discharge is computed for both catchments since REMO produces more precipitation than observed. There is also an overestimation of precipitation in the ECHAM4 simulation so that the corresponding realistic discharge amounts prove that the evapotranspiration of the ECHAM4 simulation is too large in both catchments.

The simulated inflows show also that the snowmelt in spring occurs too late in the REMO simulations (especially for the Bothnian Bay), which is based on the erroneous simulation of the 2m-temperature. The 2m-temperature is generally simulated too cold throughout the year and the rise above the freezing point in spring occurs about 1 month too late in both catchments. Contrary to this ECHAM4 simulates the snowmelt in the Bothnian Sea catchment too early. In both regions the snowmelt of REMO is about one month later than the snowmelt of ECHAM4.

In this study, the external boundary conditions of REMO were defined by an atmospheric model simulation, the errors of which may be transported into the climate patterns of the REMO region. In order to exclude any systematic errors from atmospheric model simulations, high quality external boundary conditions from analyses should be used in validation exercises which will be done in the future.

Since problems in the simulated hydrological cycle of global and regional climate models may most likely be related to systematic errors in the general circulation, future model improvements should focus on the correct representation of the atmospheric general circulation in both REMO and ECHAM4. For regional climate models, actual analysed data should be used as external spatial boundary conditions.

In the near future longer climate simulations with REMO using ECHAM4 physics and the limited area model HIRHAM4 will be done. The HD model will be applied to these simulations and the simulated inflows into the Baltic Sea will be also compared to the results presented in this paper. A further improvement of the HD model parameterizations using other gridbox characteristics may be achieved if new or improved global datasets become available at 0.5˚ resolution.

Acknowledgements

We thank Bengt Carlsson from the Swedish Meteorological and Hydrological Institute for the provision of hydrological data related to the Baltic Sea catchment. Parts of the data are described by *Bergström and Carlsson* (1993) and *Bergström et al.* (1996). We thank Daniela Jacob from the MPI and Ralf Podzun from the DKRZ for the provision of the REMO model data.

References

BALTEX (1995) Baltic sea experiment, BALTEX. Initial implementation plan. International BALTEX Secretariat. Publ. No. 2, Geesthacht

Bengtsson, L., Arpe, K., Roeckner, E., and Schulzweida, U. (1996) Climate predictability experiments with a general circulation model, *Clim. Dyn.* 12, pp. 261-278

Bergström, S. and Carlsson, B. (1993) Hydrology of the Baltic Basin, Swedish Meteorological and Hydrological Institute Report No. 7

Bergström, S., Carlsson, B., and Graham, L.P. (1996) Modeling the water balance of the Baltic Basin - preliminary results, XIX Nordic Hydrological Conference - Akureyri, August 1996

Christensen, J.H., Christensen, O.B., Lopez, P., van Meijgaard, E., and Botzet, M. (1996) The HIRHAM 4 regional atmospheric climate model, DMI Scientific Report 96-4 (Available from DMI, Lyngbyvej 100, DK-2100 Copenhagen Ø, Denmark)

Christensen, O.B., Christensen, J.H., Machenhauer, B., and Botzet, M. (1998) Very-high resolution climate simulations over Scandinavia. Present climate, *J. Climate* (in press)

CIA (1992) CIA world data bank II, Public domain dataset

Dümenil, L., and Todini, E. (1992) A rainfall-runoff scheme for use in the Hamburg climate model, In: J.P. Kane (Ed.), Advances in Theoretical Hydrology - a Tribute to James Dooge, Elsevier Science Publishers, p. 129-157

Edwards, M.O. (1989) Global gridded elevation and bathymetry (ETOPO5). Digital raster data on a 5-minute geographic (lat/long) 2160*4320 (centroid-registered) grid. NOAA National Geophysical Data Center, Boulder, Colorado

Foster, D.J., and Davy, R.D. (1988) Global Snow Depth Climatology, USAFETAC/TN-88/006, Scott Air Force Base, Illinois

Hagemann, S. (1998) Entwicklung einer Parameterisierung des lateralen Abflusses für Landflächen auf der globalen Skala, Examensarbeit 52, Max-Planck-Institute for Meteorology, Hamburg, Germany

Hagemann, S., and Dümenil, L. (1998) A parameterization of the lateral waterflow for the global scale, *Clim. Dyn.* 14 (1), pp. 17-31

Hagemann, S., and Dümenil, L. (1998b) Comparison of two global wetlands datasets using a global hydrological discharge model. Submitted to *Hydrology and Earth System Sciences*

Jacob, D., and Podzun, R. (1997) Sensitivity studies with the regional climate model REMO, *Meteorology and Atmospheric Physics* 63 , pp. 119-129

Legates, D.R, and Wilmott, C.J. (1990) Mean seasonal and spatial variability in global surface air temperature, *Theor. Appl. Climatol.*, Vol. 41, pp. 11-21

Machenhauer, B., Windelband, M., Botzet, M., Jones, R.G., Déqué, M. (1996) Validation of present-day regional climate simulations over Europe: Nested LAM and variable resolution global model simulations with observed or mixed layer ocean boundary conditions, MPI Report No. 191, Max-Planck-Institute for Meteorology, Hamburg

Machenhauer, B., Windelband, M., Botzet, M., Christensen, J.H., Déqué, M., Jones, R.G., Ruti, P.M., and Visconti, G. (1998) Validation and analysis of regional present-day climate and climate change simulations over Europe, MPI Report No. 275, Max-Planck-Institute for Meteorology, Hamburg

Majewski, D., and Schrodin, R. (1994) Short description of the Europa-Modell (EM) and Deutschland-Modell (DM) of the DWD, *Quaterly Bulletin*

Meeson, B.W., Corprew, F.E., McManus, J.M.P., Myers, D.M., Closs, J.W., Sun, K.-J., Sunday, D.J., and Sellers, P.J. (1995) ISLSCP initiative I - global data sets for land-Atmosphere models, 1987-1988. Volumes 1-5. Published on CD by NASA

Miller, J.R., Russell, G.L., and Caliri, G. (1994) Continental scale river flow in climate models, *J. Climate*, Vol. 7, pp. 914-928

Peixoto, J.P. (1993) Atmospheric energetics and the water cycle, In E. Raschke and D. Jacob (Ed.), Energy and Water Cycles in the Climate System, NATO ASI Series, Vol. I 5, Springer-Verlag Berlin Heidelberg

Roeckner, E. , Arpe, K., Bengtsson, L., Brinkop, S., Dümenil, L., Esch, M., Kirk, E., Lunkeit, F., Ponater, M., Rockel, B., Sausen, R., Schlese, U., Schubert, S., and Windelband, M. (1992) Simulation of the present-day climate with the ECHAM Model: impact of model physics and resolution, MPI Report No. 93, Max-Planck-Institute for Meteorology, Hamburg

Roeckner, E., Arpe, K., Bengtsson, L., Christoph, M., Claussen, M., Dümenil, L., Esch, M., Giorgetta, M., Schlese, U., and Schulzweida, U. (1996) The atmospheric general circulation model ECHAM-4: model description and simulation of present-day climate, MPI Report No. 218, Max-Planck-Institute for Meteorology, Hamburg

Roesch, A., Schulz, J.-P., and Wild, M. (1997) Comparison and sensitivity studies of the land-surface schemes in the ECHAM general circulation model and the Europa-Modell, MPI Report No. 244, Max-Planck-Institute for Meteorology, Hamburg

Rudolf, B., Hauschild, H., Rüth, W., and Schneider, U. (1996) Comparison of raingauge analyses, satellite-based precipitation estimates and forecast model results, *Adv. Space. Res.* 7, pp. 53-62

US Army Corps of Engineers (1994) Construction Engineering Research Laboratory, Global grass II - fifty global coverage maps, CD-ROM, Remote Sensing Center at Rutgers University

Wild, M.A., Dümenil, L., and Schulz, J.-P. (1996) Regional climate simulation with a high resolution GCM: surface hydrology, *Clim. Dyn.* 12, pp. 755-774

WMO (World Meteorological Organization) (1988) Concept of the Global Energy and Water Cycle Experiment. Technical report, WCRP-5, WMO/TD No. 215, Geneva, Switzerland